Limnol. Oceanogr., 49(4), 2004, 940–952

Quantification of marine snow fragmentation by swimming euphausiids

Sarah Goldthwait
Department of Ecology, Evolution, and Marine Biology, University of California, Santa Barbara, California 93106

Jeannette Yen and Jason Brown
School of Biology, Georgia Institute of Technology, Atlanta, Georgia 30332

Alice Alldredge
Department of Ecology, Evolution, and Marine Biology, University of California, Santa Barbara, California 93106

Abstract

Sinking of marine snow is a major mechanism of particulate carbon transport from surface waters to the seafloor. Any process altering the abundance or size of marine snow influences carbon flux and food availability to pelagic and benthic organisms. We explored whether zooplankton can alter carbon transport by a new mechanism—physical fragmentation of marine snow. The fluid stress created around the appendages of swimming *Euphausia pacifica* is capable of fragmenting a single aggregate into multiple, smaller aggregates. The reduced size and slower sinking rate of the daughter aggregates may increase their residence time in the water column, promoting decomposition and decreasing particle flux to depth. To determine the importance of fragmentation, tethered and free-swimming euphausiids were videotaped in the presence of marine snow representing a range of aggregate strengths, sizes, and ages. Image analysis was used to characterize the particles prior to and following fragmentation and to determine the area of influence around a single euphausiid. Tethered euphausiids pulled in particles from an average of 6.7 mm away, and most aggregates were fragmented in either the region of the rapidly beating pleopods or in the high-velocity jet that forms off the tail. Euphausiids were capable of fragmenting all aggregate types and produced an average of 7.3 daughter particles, with 60% of these daughter particles remaining within the marine snow size class (>0.5 mm). Thus, physical fragmentation by swimming euphausiids increases the abundance of marine snow while decreasing overall marine snow mass. This novel process, which alters particle size structure without loss of total particulate organic carbon (POC), will be important in upwelling regions where euphausiids are the dominant macrozooplankton migrators.

Macroscopic organic aggregates >0.5 mm diameter, generically categorized as marine snow, have significance in the ocean as chemically and biologically distinct microhabitats and serve as the primary transporter of surface-derived organic matter to the ocean interior and seafloor (Fowler and Knauer 1986; Asper 1987). Marine snow has diverse origins and variable composition, including phytoplankton (particularly diatoms), discarded mucous feeding structures of certain zooplankton, fecal pellets, and unidentifiable detritus (Alldredge and Silver 1988).

Marine snow can comprise as much as 60% of water column particulate organic carbon (POC) (Alldredge 1979) and is often the dominant material collected in sediment traps (Turner 2002). Below the mixed layer, the flux of POC decreases exponentially with depth (Martin et al. 1987). This decrease must arise from processes that either remove marine snow or physically fragment large, sinking particles into smaller, more slowly sinking or neutrally buoyant particles. Karl et al. (1988) described four potential mechanisms responsible for the reduction of particle flux with depth: (1) microbial decomposition, (2) microbially mediated solubilization to dissolved organic matter (DOM), (3) consumption by zooplankton, and (4) abiotic stress-induced fragmentation. Karl et al. (1988) coined the phrase ''particle decomposition paradox'' to describe the incongruity between the observed rapid decrease in POC flux with depth and the often slow rate of the four processes thought to account for removal of the sinking particle pool. However, more recent studies have found that both microbially mediated POC removal (Ploug and Grossart 1999, 2000) and particle grazing by invertebrates (Kiørboe 2000), individually, could be adequate to account for the loss of sinking particles. In a modeling study, Ruiz (1997) showed that abiotic fragmentation might also play an important role, since he was able to create observed diel patterns of particle concentration using only daily fluctuations in energy dissipation rate.

Dilling and Alldredge (2000) recently suggested a fifth potential mechanism for the decrease in POC flux with depth. In a field study they found that increased euphausiid abundance was correlated with an increase in aggregate abundance but a decrease in average aggregate size, after accounting for all other production and loss mechanisms. They demonstrated that the stress produced around the swimming legs (pleopods) of the euphausiid *Euphausia pacifica* was sufficient to cause single aggregates in an animal's vicinity to be fragmented into multiple, smaller particles. These smaller daughter particles should sink more slowly, increasing their residence time in surface waters and the potential for water column remineralization. Thus euphausiids

Acknowledgments

We thank D. Farrar for help with animal collection; M. Doall and M. Caun for laboratory assistance; and R. Ross, C. Carlson, and two anonymous reviewers for comments on the manuscript. This research was supported by NSF grant OCE-0296101.

could potentially reduce particle flux through swimming behavior alone. That zooplankton might fragment particles has been suggested previously (Banse 1990; Lampitt et al. 1990, 1993) and is supported by limited field observations (Steinberg et al. 1997).

Euphausiids have global distribution and are among the most dominant macrozooplankton migrators (Mauchline 1980). Locally, *E. pacifica* often dominate vertical migratory biomass in the California Current (Brooks and Mullin 1983) with daytime depths of about 400 m and nighttime depths of 0–100 m (Brinton 1976). Typical *E. pacifica* abundance can range from <1 to 10 animals m^{-3} with occasional swarm densities of up to 10,000 animals m^{-3} (Mackie and Mills 1983). Since all euphausiids have similar morphology with five pairs of rapidly beating pleopods, other euphausiids are also likely to be capable of aggregate fragmentation. Thus, this fragmentation process could have oceanwide importance for our understanding of particle flux. Although Dilling and Alldredge (2000) demonstrated the existence of this new mechanism of altering particle size structure, it has not yet been tested experimentally or extensively quantified.

In this study we investigated the fragmentation process using *E. pacifica* as our model euphausiid. The goal of this laboratory-based study was (1) to determine which particle attributes, including size, composition, strength, and age, most affected fragmentation, and (2) to quantify the size and number of daughter particles produced. The impact of euphausiid size and distance from an aggregate on the resulting daughter particle size spectra was also determined.

Methods

Euphausia pacifica were collected at night in the Santa Barbara Channel (SB Channel), California (34°19′N, 119°52′W) using a 1 m diameter, 335-μm mesh plankton net in surface waters (25–100 m). Animals were immediately transferred into surface seawater and maintained at 13°C on a diet of brine shrimp larvae (Lasker and Theilacker 1965). Experiments were conducted within 2 weeks of collection and used only actively swimming animals that appeared to be in good health. Animals were tethered for most trials due to difficulties of filming free-swimming animals interacting with snow (both due to animal behavior in tanks and snow sinking out of the system). However, particle image velocimetry (PIV) data from untethered animals were used to verify results from tethered studies. Euphausiids (size range 13.6 to 24.3 mm) were tethered by means of a fine gauge wire superglued to the dorsal surface of the carapace just posterior to the eyes. The animal was oriented upward at about 20° from horizontal and then suspended in a Plexiglas tank ($\sim$1 liter in volume) filled with surface seawater. This angle was chosen because free-swimming animals hover at a fixed angle of about 20° (Miyashita et al. 1996). Marine snow was gently added near the tank surface with a pipette and allowed to sink naturally past the animal. An effort was made to deliver a variety of particle sizes, all >0.5 mm, from all directions.

Experimental design—We used natural marine snow collected from different locations and on different dates in an attempt to represent the well-documented variability in aggregate composition (Alldredge and Silver 1988). Natural marine snow was collected in the SB Channel via self-contained underwater breathing apparatus (SCUBA) in 50-ml bulk aggregate slurry syringes (about 50 particles per syringe; Alldredge 1991). Syringe contents were gently decanted into a 250-ml bottle and reaggregated on a rolling table at 13°C (Shanks and Edmondson 1989). Natural marine snow, collected on 25 June 2000 (15 m) and 14 May 2002 (20 m) in the SB Channel, was used within 0–6 d of collection. We also tested (within 2–6 d) the fragmentation of marine snow aggregates that had been collected from a surface nighttime zooplankton tow on 16 May 2002 in Puget Sound, Washington, and then been reaggregated.

To assess fragmentation over a greater range of aggregate strengths, artificial marine snow was made on a rolling table from cultures of *Skeletonema costatum, Chaetoceros neogracilis, Nitzschia angularis, Coscinodiscus radiatus, Cylindrotheca fusiformis, Navicula pelliculosa, Thalassiosira weissflogii,* and a mixed (*C. neogracilis*/*T. weissflogii*) diatom culture. These species represent some of the dominant particle-forming genera in upwelling systems and generated marine snow over a range of particle strengths (Alldredge et al. 1990) and sizes. Cultures were grown in f/2 media and transferred to a rolling table in stationary growth phase to promote aggregation.

The effects of aggregate age on fragmentation were determined for marine snow collected individually in 6-ml polypropylene cylinders on the morning of 3 August 2002 (13 m) in the SB Channel (34°16′N, 119°53′W). Fragmentation trials were conducted daily at dusk from day 0 (3 August 2002) through day 3 (6 August 2002) using a different, but similarly sized, animal each day. We used a 4-d time course, since this is the interval over which euphausiids migrating from 300 m to the surface would be most likely to encounter these aggregates based on sinking speeds of 50–75 m d^{-1} (Alldredge and Gotschalk 1988).

Camera systems for marine snow trials—Different camera systems were used during the three distinct time intervals over which animals were filmed with aggregates. All systems visualized two view planes oriented at a 90° angle to provide three-dimensional location data for the animals and aggregates. System 1 (27–30 June 2000) had two low-light Pulnix TM-745 cameras with one camera using Schlieren optics (after Strickler 1998) and the other using a fiber-optic light source. All trials for *S. costatum, C. radiatus,* and 25 June 2000 SB Channel marine snow were conducted with system 1. System 2 (16–20 May 2002) used Schlieren optics and a single Pulnix TM-745 camera with an overlapping split screen output (Strickler 1998). The Plexiglas tank containing the animal was partially submersed in a recirculating water jacket set at 12°C. System 2 provided the bulk of the dataset, including all trials for *C. neogracilis, N. angularis, C. fusiformis, N. pelliculosa, T. weissflogii,* mixed diatom culture, Puget Sound marine snow, and 14 May 2002 SB Channel marine snow. For systems 1 and 2, the Schlieren optics images were used for particle assessments. Thus, particle size and thresholding were not system specific, and data from these two systems could be pooled. System 3 (3–6

August 2002) was a shipboard system with two Pulnix TM-745 cameras illuminated by fiber-optic lighting. System 3 was used solely for the snow aging study. Owing to the difference between system 3 and systems 1 and 2, data from the snow aging study were not combined with data from previous trials. Thus, data for all particles do not include trials from system 3.

Data analysis for marine snow trials—For all (non-PIV) systems, images were recorded onto Super VHS videotapes using a Panasonic AG-1960 Super VHS video cassette recorder connected to a Horita TRG-50 SMPTE time code generator. Videotapes were digitized using an Adaptec 2930 small computer system interface (SCSI) frame grabber board, and Metamorph image analysis software (Universal Imaging) was used to size, count, and track particles. Only particles >2 pixels were analyzed, typically resulting in a size cutoff ~250 μm in diameter. Daughter particles smaller than this size cutoff were counted but not sized.

Two distance measurements were determined using a central point on the test euphausiid for reference. This point was defined as the posterior end of the carapace, midway through the animal's dorsal–ventral axis. Distance drawn in refers to the distance at which the particle changed velocity or direction in response to a euphausiid's swimming current. Distance fragmented refers to the distance at which the particle was initially fragmented. If multiple fragmentation events occurred for the same particle, only the location of the first event was used.

In order to determine the percentage of particles that fragmented, we assessed the fate of all particles within a 6-mm radius of tethered animals. An average of 85 particles of each snow type (spanning the size range of the snow type) was tested. The 6-mm radius was based on the average distance from which euphausiids could draw in and fragment particles as determined in this study (*see results section*). The percentage of particles fragmented was determined for euphausiids representing the range of adult animal sizes.

Parent and daughter particle sizes were normalized via log transformation prior to statistical analysis. Regression analysis was used to compare variables with the exception of animal size data, which were assessed using one-way analysis of variance (ANOVA) with a post hoc least squared difference (LSD) test. Statistical analyses were conducted separately on each different type of aggregate. Reported results for all particles include all aggregate types, regardless of whether the aggregate type showed significant differences when analyzed individually. Comparisons of parent versus total daughter aggregate equivalent spherical volume (ESV) and equivalent spherical surface area (ESSA) were made using a paired-sample *t*-test.

Particle image velocimetry—Particle image velocimetry (PIV) (Westerweel 1997; Raffel et al. 1998) was used to measure the velocity field around tethered (Yen et al. 2003) and free-swimming *E. pacifica* and to assess the stress field responsible for aggregate fragmentation. This well-established and noninvasive optical technique has been used previously to measure the velocity field around zooplankton (e.g., van Duren et al. 1998, 2003). A sheet of pulsed laser light was used to illuminate a flow field seeded with flow-tracing particles (diameter of 1–10 μm). The laser used for the tethered animal PIV was a dual Neodymium: Yttrium-Aluminum-Garnet (Nd:YAG) system emitting at 532 nm; for the measurements with free-swimming krill, pulsed laser light at 808 nm was shaped into a suitable sheet. This infrared light did not cause any changes in the animals' behavior. A digital video camera, synchronized with the laser, captured a series of images of the illuminated plane at known time intervals. Small, corresponding subregions of two sequential images were processed on a personal computer by digital two-dimensional cross correlation to determine the displacement of the particles within the subregion.

The displacement at multiple (e.g., over 3000 for the tethered animal) points at a given time can be calculated by repeating the two-dimensional cross correlation at regular intervals over the entire field of view. The instantaneous velocity field is then generated by dividing each displacement measurement by the time elapsed between exposures. At this point the stress field may be computed. The state of stress at each point is specified by the stress tensor which, for a fluid, can be broken down into pressure and viscous terms. The viscous term is a tensor whose six independent components are functions of derivatives of the velocity field. Taking p as the pressure; μ as the absolute viscosity; and u, v, and w as the components of velocity in the x, y, and z directions, respectively, the stress tensor may be written as

$$-p\begin{pmatrix}1 & 0 & 0\\ 0 & 1 & 0\\ 0 & 0 & 1\end{pmatrix} + 2\mu\begin{bmatrix}\dfrac{\partial u}{\partial x} & \dfrac{1}{2}\left(\dfrac{\partial u}{\partial y}+\dfrac{\partial v}{\partial x}\right) & \dfrac{1}{2}\left(\dfrac{\partial w}{\partial x}+\dfrac{\partial u}{\partial z}\right)\\ \dfrac{1}{2}\left(\dfrac{\partial u}{\partial y}+\dfrac{\partial v}{\partial x}\right) & \dfrac{\partial v}{\partial y} & \dfrac{1}{2}\left(\dfrac{\partial w}{\partial y}+\dfrac{\partial v}{\partial z}\right)\\ \dfrac{1}{2}\left(\dfrac{\partial w}{\partial x}+\dfrac{\partial u}{\partial z}\right) & \dfrac{1}{2}\left(\dfrac{\partial w}{\partial y}+\dfrac{\partial v}{\partial z}\right) & \dfrac{\partial w}{\partial z}\end{bmatrix} \quad (1)$$

Terms on the diagonals are the normal stresses, and off-diagonal terms are the shear stresses (Schlichting 1979).

PIV, as practiced here, measures only the u and v components of (in plane) velocity, and thus only three independent components of the viscous stress tensor may be determined directly. A fourth component, $\partial w/\partial z$, can be calculated for an incompressible fluid by invoking the conservation of mass and indicates the presence of out-of-plane flow. The pressure cannot, in general, be estimated from PIV data. However, in the case of incompressible, steady, two-dimensional flow, the pressure field may be determined by invoking the appropriate form of the Navier–Stokes equations (Raffel et al. 1998). The flowfield produced by krill was neither steady nor two dimensional, particularly near the pleopods, so pressure remains unknown, and only the instantaneous viscous stress tensor was calculated using the u and v components found via PIV:

$$2\mu\begin{bmatrix} \dfrac{\partial u}{\partial x} & \dfrac{1}{2}\left(\dfrac{\partial u}{\partial y}+\dfrac{\partial v}{\partial x}\right) \\ \dfrac{1}{2}\left(\dfrac{\partial u}{\partial y}+\dfrac{\partial v}{\partial x}\right) & \dfrac{\partial v}{\partial y} \end{bmatrix} \quad (2)$$

In order to reduce this tensor to a single number representative of the state of stress at a point, the instantaneous von Mises stress was computed at every grid point over the field. The von Mises stress is generally used as part of a criterion of structural failure (e.g., Buchanan 1988; Shigley and Mischke 1989; Bickford 1993), roughly analogous to the present context, and is typically calculated as follows. For any symmetric tensor in an arbitrary orthogonal coordinate system, such as the viscous stress tensor, a set of orthogonal coordinate axes can be found such that when the tensor is transformed (rotated) into these axes the shear components of the tensor vanish, leaving only transformed normal stresses. The special axes in which this occurs are called the principal axes, and the normal stresses in this coordinate system are called the principal stresses. In the case of the viscous stress tensor derived from PIV data, the two principal stresses are given by

$$\bar{\sigma}_{1,2} = \mu\left[\frac{\partial u}{\partial x}+\frac{\partial v}{\partial y} \pm \sqrt{\left(\frac{\partial u}{\partial x}-\frac{\partial v}{\partial y}\right)^2+\left(\frac{\partial u}{\partial y}+\frac{\partial v}{\partial x}\right)^2}\right] \quad (3)$$

From these principal stresses, the von Mises stress is then computed by

$$\sqrt{\frac{1}{2}[(\bar{\sigma}_1-\bar{\sigma}_2)^2+(\bar{\sigma}_2)^2+(\bar{\sigma}_1)^2]} \quad (4)$$

Results

Tethered animals generally swam continuously and often attempted to feed as seen by expansions of the feeding basket. Following filming, many animals dislodged themselves from the tether and continued to live for several days, suggesting that tethering did not damage the carapace of the animal. Observations of tethered and free-swimming animals in particle fields indicated that particles were drawn toward the animal laterally and moved most rapidly in the region of the swimming appendages (pleopods; Fig. 1A,B). A downward high-velocity jet formed off the tail region of the animal. Maps of stress around tethered animals indicated von Mises stresses as high as 1.4 dyn cm^{-2} in the pleopod region and 0.2 dyn cm^{-2} off the tail (Fig. 1C,D). Similar maps for free-swimming specimens show von Mises stresses of up to 0.6 dyn cm^{-2} in the pleopod region and 0.2 dyn cm^{-2} at 3 cm off the tail (Yen unpubl. data).

Description of parent aggregates—We analyzed the fragmentation of 786 individual aggregates representing natural marine snow collected on three distinct dates, as well as seven different types of artificial marine snow made from diatom cultures. Snow collected on 24 June 2000 was very loosely aggregated, dinoflagellate snow with diatom setae and some fecal matter, differing from snow collected on 14 May 2002 that was composed mainly of miscellaneous detrital material. Marine snow from the zooplankton tow in Puget Sound on 16 May 2002 consisted of large (~4 mm diameter), comet shaped aggregates composed of detrital and fecal material as well as pieces of crustacean carapaces. All naturally collected aggregates also contained unidentifiable detritus. The sizes of the aggregates ranged from 0.5 to 14.7 mm in diameter and 0.02 to 218 mm^3 in equivalent spherical volume (ESV) (Table 1). Aggregate size is expressed here as maximum diameter, since this is the largest dimension over which eddy motion can interact with a particle (Alldredge et al. 1990). Parent particle refers to the original particle prior to fragmentation into multiple daughter particles. All parent particles were within the marine snow size class designation (i.e., >0.5 mm diameter). The size class distribution of parent particles indicated that the majority of these particles were between 0.8 to 2.5 mm in diameter. Natural marine snow aggregates were generally larger than laboratory-made aggregates, although *C. fusiformis* and *N. angularis* also formed large particles (Table 1).

Percent of aggregates fragmented—Depending on particle type and animal size, 16–100% (average = 60%) of aggregates fragmented within a 6-mm radius of the animal (Table 2). Aggregates that did not fragment but were entrained by the feeding current increased very slightly in diameter (by 71 μm on average; paired-sample *t*-test, $p < 0.05$) but had no significant change in equivalent spherical volume (ESV; paired-sample *t*-test). The increased diameter likely resulted from a slight stretching of the aggregate due to shearing as it passed through the current generated by the euphausiid. Most particles that did not fragment were in the smallest marine snow size class (0.5–0.6 mm). The more fragile aggregate types such as the mixed diatom culture, *C. neogracilis*, *N. pelliculosa*, and Puget Sound marine snow fragmented more readily than stronger aggregates, notably *C. fusiformis*, *N. angularis*, and May 2002 SB Channel snow. For the same snow types, larger animals tended to fragment a greater percentage of aggregates (Table 2).

Distance—The majority of particles were drawn in from above the euphausiids, likely an artifact of particles being released at the water surface (Fig. 2A,B). Particles that were later fragmented were drawn in from an average of 6.7 mm ± 3.5 mm. This number may be considered the mean effective radius of fragmentation for a swimming *E. pacifica*. However, particles may be drawn in from distances as great as 40 mm. The majority of particles (>70%) were fragmented in the region of the pleopods (Fig. 2C), where the highest stresses are generated (Fig. 1C). However, particles can also be fragmented as far away as 37 mm from the animal, typically in the high-energy jet that forms off of the tail region.

Description of daughter aggregates—The 786 parent particles fragmented into 5757 daughter particles, with each parent particle producing an average of 7.3 daughter particles (range 2–120). A parent particle splitting into two daughter particles was most common (28.4% of cases), while trials with three to nine daughter particles accounted for an-

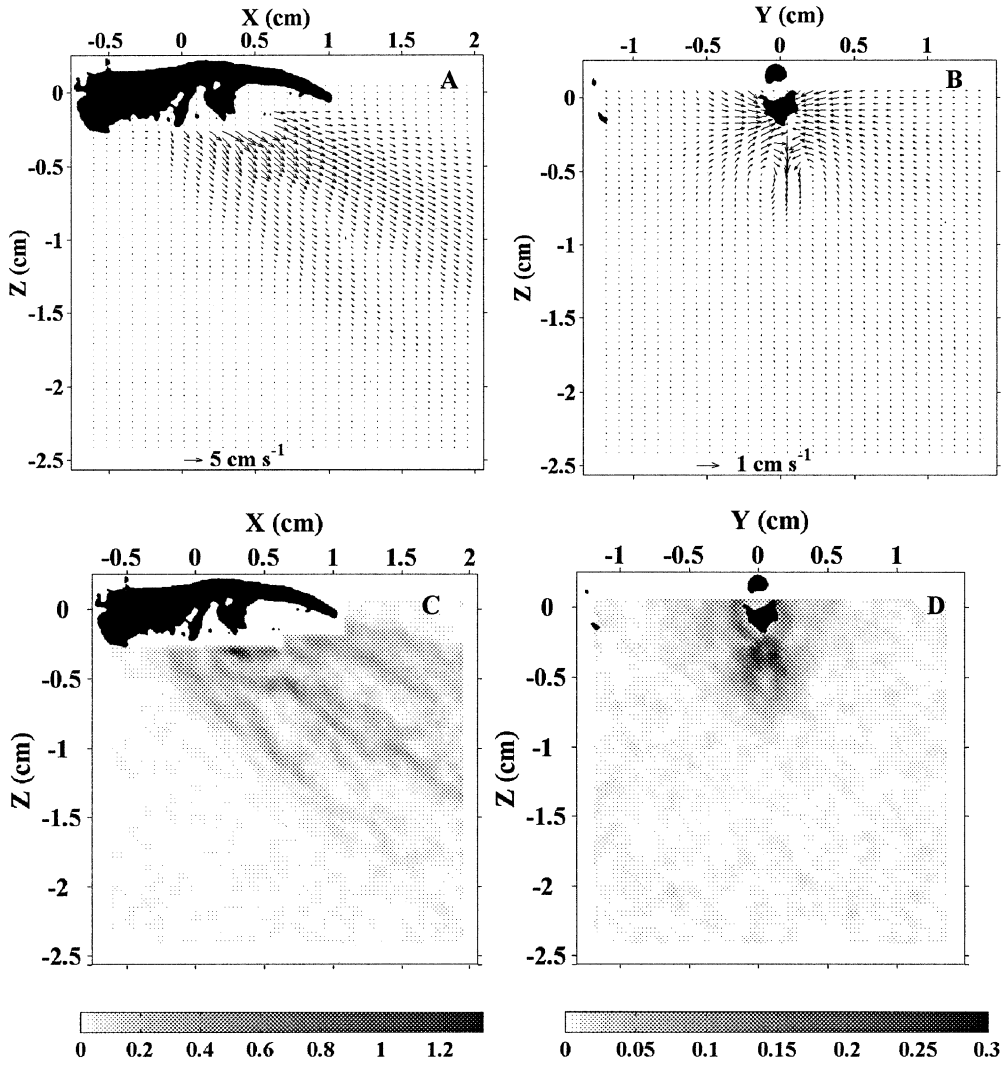

Fig. 1. Sample instantaneous PIV velocity fields for a tethered euphausiid shown in the (A) side-view and (B) head-on plane. For each field, half of the vectors are shown in order to improve clarity. Sample instantaneous von Mises stress fields, in dyn cm^{-2}, in the (C) side-view and (D) head-on plane.

other 52.8% (Fig. 3). The size class distribution of the daughter particles shifted dramatically toward smaller size classes, with 40% of daughter particles being less than 0.5 mm (Fig. 4). More fragile aggregates such as Puget Sound aggregates, *C. radiatus*, *N. pelliculosa*, and the mixed diatom culture tended to produce greater numbers of daughter particles with a larger percentage of daughter particles being lost from the marine snow size range (Table 1). SB Channel aggregates from both dates produced similar numbers of daughter particles with ~35% of daughter particles being less than 0.5 mm. Even though the average diameter of daughter particles was significantly less (paired-sample *t*-test, $t = 41.583$, df = 785, $p < 0.001$) than that of the parent particle, most (60%) daughter particles and >90% of daughter ESV remained within the marine snow size range designation, and thus there was an overall increase in the abundance of marine snow particles due to the fragmentation process (Table 1).

Parent particle size—The number of daughter particles increased exponentially with increasing parent particle size for all particle types (regression, $F = 228.838$, $r^2 = 0.226$, $p < 0.001$), although the number of daughter particles produced was quite variable for a given particle size class (Fig. 5). Average daughter ESV was also positively related (regression, $F = 957.087$, $r^2 = 0.549$, $p < 0.001$) to parent ESV for all snow types except Puget Sound marine snow (Fig. 6A). While a strong positive association (regression, $F = 4254.714$, $r^2 = 0.844$, $p < 0.001$) was found between parent ESV and the sum of the daughter particle ESVs, parent ESV was significantly greater (by ~1.9 mm^3 ESV, 1.5 mm diameter) than the combined ESV for all daughter particles produced (paired-sample *t*-test, $t = 14.237$, df = 785, $p < 0.001$), indicating that some particle volume was lost during fragmentation. In contrast, total daughter particle equivalent spherical surface area (ESSA) was significantly greater (by ~14%) than that of the parent particle (Fig. 6B;

Table 1. Summary of the fragmentation outcomes for all aggregate types combined and by aggregate type. This table shows the number and size of parent particles that fragmented and the resultant number and size of all daughter particles produced. The percentage of daughter particle abundance in relation to the marine snow size cutoff (>0.5 mm) is shown.

Aggregate type	No. parent particles	No. daughter particles (all sizes)	Average No. daughter parent^{-1}	Average parent ESV (mm^3)	Average daughter ESV (mm^3)	% daughter particles <0.5 mm	% daughter particles >0.5 mm
All aggregates	786	5757	7.3±10.2	7.7±18.1	0.8±6.4	40	60
SB Channel marine snow (25 Jun 2000)	50	312	6.2±5.9	11.1±19.3	1.4±2.4	33	67
SB Channel marine snow (14 May 2002)	100	537	5.4±5.5	9.1±16.9	1.1±2.0	38	62
Puget Sound marine snow (16 May 2002)	28	369	13.2±21.8	32.3±54.7	6.0±23.9	63	37
Skeletonema costatum	113	648	5.7±5.2	5.9±9.8	0.9±1.5	26	74
Coscinodiscus radiatus	32	264	8.3±6.8	2.7±4.5	0.2±1.1	59	41
Chaetoceros neogracilis	79	341	4.3±4.7	2.5±10.2	0.3±0.6	43	57
Mixed culture (*C. neog./ T. weissflogii*)	102	1212	11.9±11.2	3.0±4.6	0.19±0.3	46	54
Nitzschia angularis	107	555	5.2±6.0	12.9±24.2	2.8±6.5	14	86
Navicula pelliculosa	109	1303	12.0±17.4	4.1±8.6	0.25±0.5	48	52
Cylindrotheca fusiformis	66	216	3.3±2.6	9.1±13.2	2.7±4.8	27	73

paired-sample *t*-test, $t = -10.226$, df = 785, $p < 0.001$). Particle surface area is a key parameter since it may be important in mediating absolute attached bacterial abundance and thus particle remineralization rates (Ploug et al. 1999).

The size of the parent particle affected both the distance from which the particle could be drawn in and where it fragmented relative to the animal. Parent particle size was positively correlated with the distance from which it was drawn in for all particles combined (regression, $F = 34.192$, $r^2 = 0.050$, $p < 0.001$), but this relationship did not hold for *S. costatum, N. pelliculosa, C. fusiformis,* and SB Channel (25 June 2000) marine snow when analyzed individually. Larger particles generally fragmented farther away from the animal (Fig. 7A) (regression, $F = 8.299$, $r^2 = 0.011$, $p = 0.004$). While these relationships are significant, they accounted for little of the variability observed in the distance measurements.

Daughter particle size—Smaller daughter particles resulted from fragmentation events closer to the animal (regression, $F = 23.867$, $r^2 = 0.034$, $p < 0.001$; Fig. 7B), where shear stress would be highest, except for *S. costatum, N. pelliculosa, C. fusiformis,* and SB Channel (25 June 2000) marine snow when analyzed individually. Surprisingly, distance at fragmentation did not affect the number of daughters produced for all particles combined, although this trend was apparent for *N. pelliculosa, N. angularis,* and Puget Sound marine snow when analyzed individually. For these snow types, greater numbers of daughter particles were produced for fragmentation events closer to the animal.

Table 2. Percentage of aggregates that fragmented (within a 6-mm radius of a central point on the test euphausiid) by aggregate type and animal size. Animal effective radius (±1 SD) is indicated in parentheses and corresponds to the average distance from which the animal was capable of drawing in and fragmenting aggregates. Santa Barbara (SB) Channel and Puget Sound snow are natural, field collected aggregates. All other aggregates were made from laboratory cultures.

	Euphausiid length (effective radius)			
Aggregate type	% 13.60 mm (4.9±2.0 mm)	% 18.01 mm (7.3±2.4 mm)	% 18.70 mm (5.8±3.7 mm)	% 24.34 mm (7.0±2.8 mm)
SB Channel snow (25 Jun 2000)		65		
SB Channel snow (14 May 2002)	33		48	57
Puget Sound snow (16 May 2002)	67	41		100
Skeletonema costatum			51	
Coscinodiscus radiatus			85	
Chaetoceros neogracilis	64	62		
Mixed culture (*C. neog./T. weissflogii*)	76	95		81
Nitzschia angularis	34	50		76
Navicula pelliculosa	46	73		86
Cylindrotheca fusiformis	16	28		78
Mean	48	59	61	80

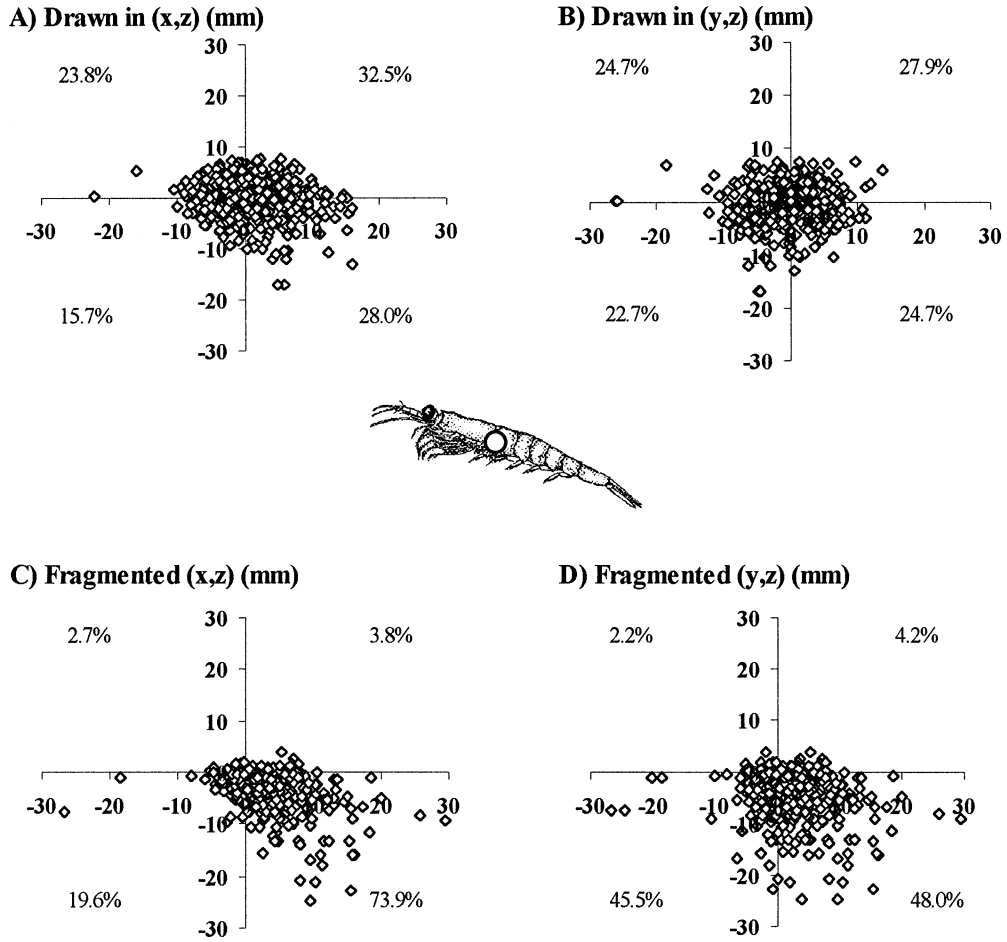

Fig. 2. Distance plots in space where (0, 0) is the central point on the tethered euphausiid, as pictured (drawing after Brinton and Wyllie 1976). Location from which particles were drawn in for the (A) side-view and (B) head-on plane. Location where particles fragmented for the (C) side-view and (D) head-on plane. Percentage of particles in each quadrant noted.

Animal size—For all particles combined, animal length significantly affected the number of daughters produced (ANOVA, $F_8 = 5.762$, $p < 0.001$), with fragmentation by larger animals producing more daughter particles (Table 3).

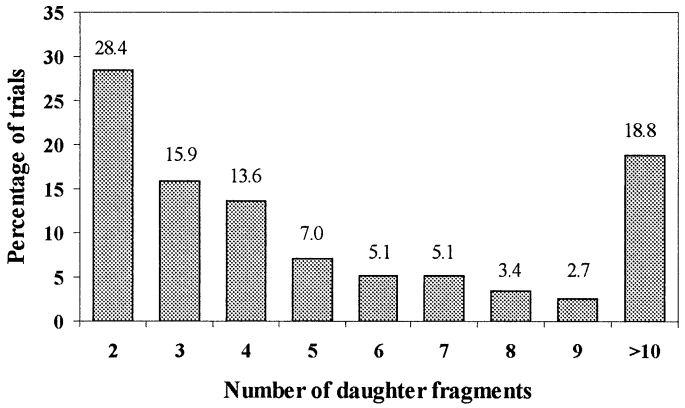

Fig. 3. Frequency distribution of the number of daughter fragments produced for all trials (except snow aging) that resulted in fragmentation. Percent values above each bar ($n = 786$).

However, this trend is driven solely by the largest animal, which produced significantly more daughter particles than all other animals tested (LSD, $p < 0.05$). Average daughter diameter and ESV differed significantly with animal length (ANOVA, $F_8 = 4.959$, $p < 0.001$), with the largest animal producing the smallest daughter particles (LSD, $p < 0.05$). The effective radius, or average distance from which particles were drawn in, varied significantly with animal size (ANOVA, $F_8 = 15.138$, $p < 0.001$), although, surprisingly, the greatest effective radii were found for two midsize animals rather than for the largest animals tested (Table 3, shown in bold). Longer animals would be expected to create larger, more energetic flow fields capable of drawing particles in from farther away. Distance at which fragmentation occurred also varied with animal size (ANOVA, $F_8 = 6.420$, $p < 0.001$) with the same two midsize animals, on average, fragmenting particles from the greatest distance. However, the two animals larger than 23 mm were responsible for the greatest observed distance from which a particle was drawn in and fragmented, respectively.

Marine snow age—The marine snow used in the aging study was composed largely of diatoms (dominated by

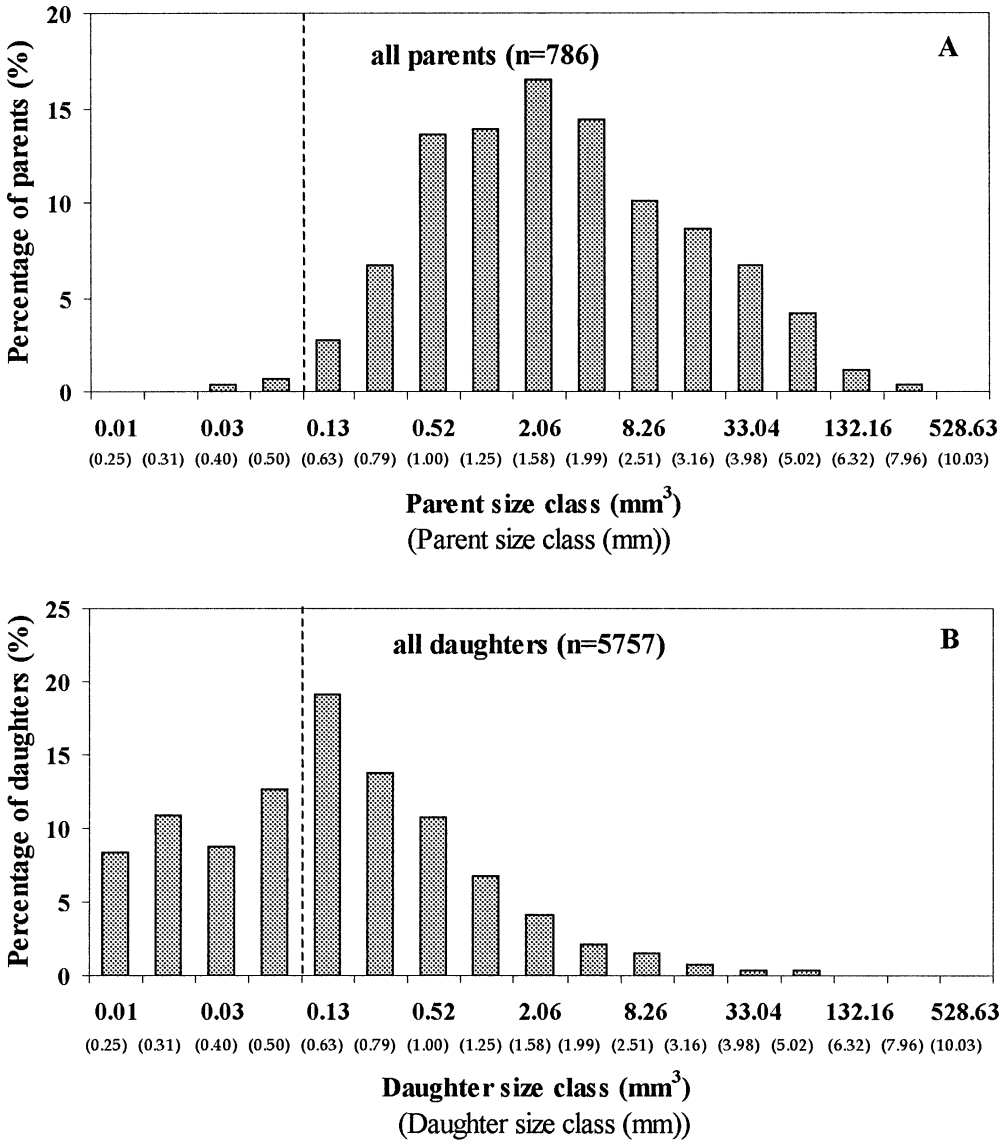

Fig. 4. Size class distribution of (A) parent aggregates and (B) daughter aggregates for all aggregate types combined. The *x*-axis is labeled with the maximum size of each bin (in equivalent spherical volume and diameter). Dotted line indicates the marine snow size cutoff (>0.5 mm).

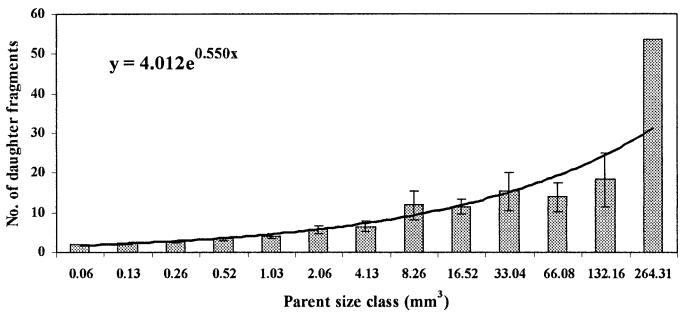

Fig. 5. Average number of daughter fragments by parent size class for all aggregate types combined. Error bars are ±1 SE (F = 228.8, r^2 = 0.226, $p < 0.001$).

Chaetoceros spp., *Nitzschia* spp., germinated diatom cysts) with some associated large fecal pellets likely produced by *E. pacifica.* The average particle diameter was 1.5 mm and did not vary throughout the time course. Neither the number of daughter particles nor the distance at fragmentation changed significantly over time. However, there was a trend toward increased fragility of the snow with time (age) as the average number of daughter particles increased from 2.9 ± 2.6 on day 0 to 6.3 ± 8.0 on day 3 (Fig. 8). Also, the percentage of particles fragmented increased from 47% on day 0 to 53% on day 3, with the largest unfragmented particle decreasing in size from 3.8 mm on day 0 to 1.4 mm on day 3. These results can be considered conservative, since the animal used on day 3 (length = 15.386 mm) was much smaller than the animal from day 0 (length = 20.528 mm). Fecal pellets associated with these marine snow aggregates

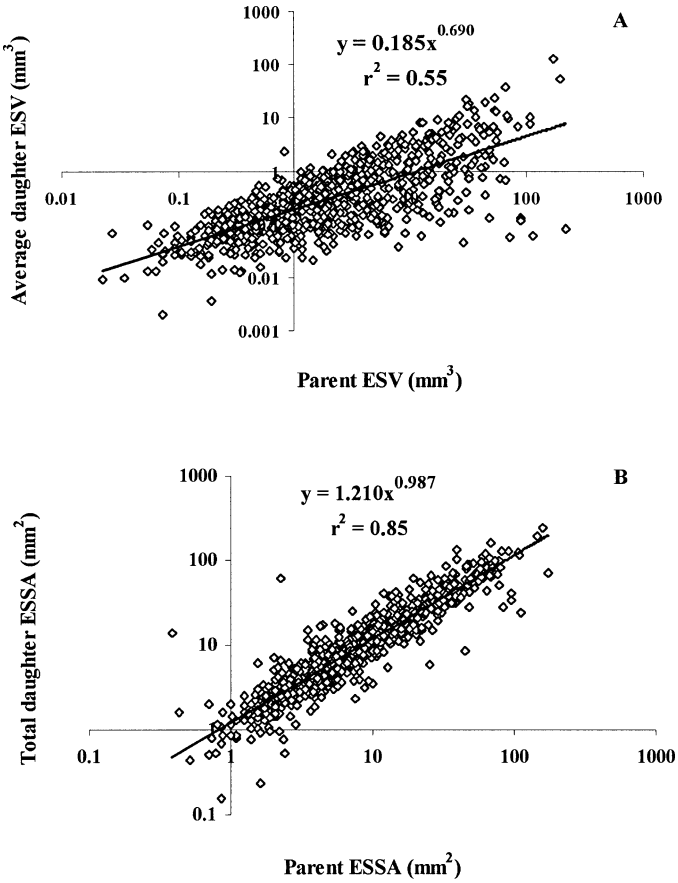

Fig. 6. (A) Comparison of average daughter equivalent spherical volume (ESV) and parent ESV for all aggregate types ($F = 957.1$, $p < 0.001$). (B) Comparison of total daughter equivalent spherical surface area (ESSA) and parent ESSA (regression, $F = 4621.475$, $p < 0.001$). Daughter particles have a greater ESSA than parent particles (paired-sample t-test, $t = -10.226$, df = 785, $p < 0.001$).

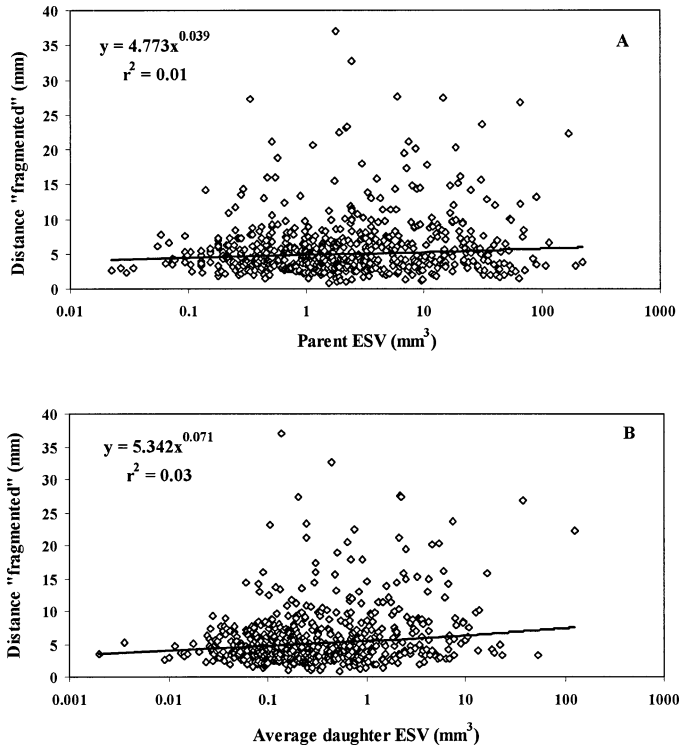

Fig. 7. Distance at which parent particles were (A) fragmented compared to parent particle equivalent spherical volume (ESV). Fragmented refers to the location of the initial fragmentation event. Distance fragmented was positively correlated with parent particle ESV ($p < 0.001$), but parent ESV accounted for little variability in the distance parameters (note low r^2 value). (B) Relationship between distance at which an aggregate was fragmented to the average daughter particle ESV. The average daughter ESV increased with increasing distance at fragmentation ($F = 8.705$, $p < 0.05$). Distances are relative to a central point on the test euphausiid.

often dissociated from the aggregates upon being pipetted into the experimental tank. We made 29 observations of animals interacting with fecal pellets (length 0.98–4.79 mm). Fecal pellets fragmented in 41.3% of cases, producing an average of 2.4 ± 0.9 daughter particles (range 2–5).

Discussion

Physical fragmentation of marine snow was proposed by Karl et al. (1988) as a potentially important process for explaining the rapid loss of sinking particles beneath the mixed layer. Disaggregation has traditionally been thought to be

Table 3. Influence of animal length on daughter particle number, diameter, and equivalent spherical volume (ESV). Average distance from which particles were drawn in and fragmented as a function of animal size is shown. One-way ANOVA found significant differences in all categories by animal size ($p<0.001$). Post hoc LSD tests found significant differences by animal length as designated by letters in superscript (a>b>c>d>e; $p<0.05$).

Animal length (mm)	Average number daughter particles	Average daughter diameter (mm)	Average daughter ESV (mm³)	Average distance drawn-in (mm) = effective radius	Average distance fragmented (mm)
13.604	6.7^{b}	1.4^{a}	2.0	4.9^{e}	4.9^{c}
16.755	5.5^{b}	1.2^{a}	0.7	6.0^{d}	6.4^{b}
17.176	5.2^{b}	1.4^{a}	1.3	**11.2**^{a}	**7.4**^{bc}
18.011	5.3^{b}	1.2^{a}	0.7	7.3^{c}	3.7^{c}
18.704	6.5^{b}	1.3^{a}	2.2	5.8^{d}	5.7^{bc}
19.054	7.9^{b}	1.3^{a}	1.1	**9.8**^{abc}	**12.2**^{a}
23.450	7.2^{b}	1.3^{a}	1.6	8.4^{b}	6.6^{b}
24.337	12.8^{a}	0.9^{b}	0.6	7.0^{c}	6.7^{b}
Mean	7.3	1.24	1.3	6.7	5.9

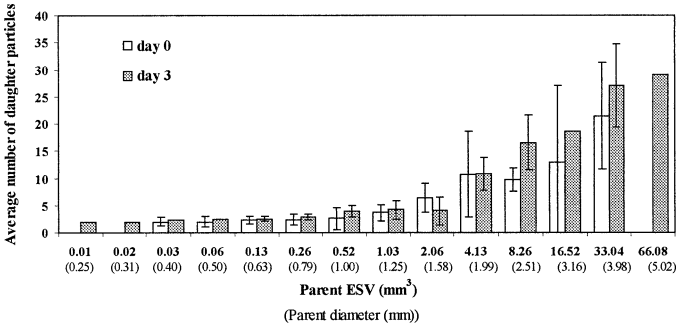

Fig. 8. Number of daughter fragments by particle size class for the first day (day 0) and last day (day 3) of the snow aging experiment using Santa Barbara Channel marine snow collected on 3 August 2002. The *x*-axis is labeled with the maximum size of each bin (in equivalent spherical volume and diameter). Error bars are ±1 SD.

mediated by abiotically produced shear stress. In a modeling study Ruiz (1997) was able to account for aggregate losses by relying only on daily fluctuations in mixed layer turbulence. However, energy dissipation rates (ranging from 10^{-9} to 7×10^{-8} m^2 s^{-3}; Ruiz 1997) were an order of magnitude less than what would be required to disrupt even the most fragile diatom aggregates (Alldredge et al. 1990). Here we have quantified a novel biotic mechanism by which marine snow could be fragmented through swimming behavior of macrozooplankton.

Three processes have been proposed to be potentially important for the breakup of marine aggregates (Parker et al. 1972): surface erosion, whereby turbulent drag erodes small daughter particles from the surface of a large parent particle; filament fracture or particle splitting, where the strength of the aggregate is related to the filament network created by attached bacteria (Alldredge et al. 1990); and instantaneous pressure fluctuations. Both modeling studies (Hill 1996) and laboratory studies using shear generated by an oscillating grid (Alldredge et al. 1990) have concluded that filament fracture is likely the dominant process for disruption of aggregates abiotically. Biotic fragmentation by macrozooplankton can best be explained by instantaneous pressure fluctuations due to differences in fluid motion across the particle surface generated by animal swimming appendages. This process generates a much higher average number of similarly sized daughter particles (7.3 in this study) than filament fracture, where most aggregates fragment into only two daughter particles (Alldredge et al. 1990).

It was not clear whether aggregate fragmentation resulting from swimming-induced shear stress would increase or decrease the marine snow pool. In this study we found that fragmentation by swimming euphausiids was a marine snow generating process, since roughly 60% of daughter particles remained within the marine snow size classification. However, since particles are lost to size classes smaller than marine snow, both the total particle volume and mean size of marine snow should decrease. Consistent with our lab results, euphausiid abundance in the field has been positively correlated with an increase in marine snow abundance and a decrease in mean aggregate size (Dilling and Alldredge 2000). Although we investigated aggregates large enough to be significant in sedimentation processes, euphausiids and/or other zooplankton might also be capable of fragmenting aggregates <0.5 mm in diameter by swimming and, thus, alter the sizes and dynamics of these smaller particles as well.

Euphausiids were capable of fragmenting all aggregate types tested, representing a range of aggregate strengths and sizes. Even the strongest aggregates tested, namely, *C. fusiformis* aggregates formed by benthic diatoms, were often disrupted. Natural marine snow typically fragmented less readily and into fewer daughter particles than artificial flocs made from pelagic diatoms. However, fragmentation of natural marine snow was also variable. Marine snow from Puget Sound fragmented much more readily than SB Channel snow. Puget Sound aggregates were larger in size, which can indicate older age. Even though aggregates collected from a single dive have similar composition, the proportion of compositional constituents and the history of the aggregates and their attached biota can vary. By averaging over a range of aggregate types, strengths, and sizes, our data should provide a robust quantification of fragmentation for natural systems.

Larger parent particles generally produced greater numbers of daughter particles. Marine snow, due to its fractal geometry (Logan and Wilkinson 1990; Kilps et al. 1994), is formed primarily by collisions of clusters of particles. Larger particles are generally older and result from a history of many particle collisions. Fragmentation may then release these once-separate clusters. Since these original clusters may have variable composition, it is not unreasonable to assume that the daughter particles produced during fragmentation might actually have differing densities, composition, and particulate organic carbon (POC) content. Fragmentation might also result in the release of nutrients and dissolved organic matter (DOM) known to have elevated interstitial concentrations within marine snow (Shanks and Trent 1979; Alldredge 2000).

The decrease in total daughter ESV compared to parent ESV suggests that there is a loss of particle volume during the fragmentation process. Aggregates have porosities ranging from 97% to 99.9%, depending on aggregate size and type (Alldredge and Gotschalk 1988). Fragmentation and subsequent tumbling may compact daughter particles, reducing interstitial spaces and decreasing total daughter ESV. Decreased total ESV of daughter particles might also arise from loss of mass to particle sizes under the detection limit of the camera system.

Not surprisingly, the total ESSA for daughter particles exceeded that of the parent particle. Increased surface area of daughter particles would sustain increased colonization by attached biota, particularly bacteria, since attached bacterial abundance has been related to available surface area (Ploug et al. 1999), potentially leading to higher rates of daughter particle solubilization and remineralization relative to the parent particle. Thus, fragmentation by swimming macrozooplankton might serve to retain C in surface waters both by reducing aggregate sinking rates and by enhancing attached bacterial production.

Older aggregates tended to fragment more readily and into more daughter particles than younger aggregates. Aggregate

strength might decrease with age due to solubilization and the weakening of the attachments between particle clusters or due to channels created over time by flagellates, ciliates, and small invertebrates along which the aggregate could fragment (Steinberg et al. 1997). In contrast, Alldredge et al. (1990) found that older aggregates were stronger and hypothesized that growing microbial populations produced exudates, capsular material, fimbriae, and fibrils that strengthened the aggregates. However, these two studies may have simply caught aggregates at different stages of aging. Aggregates may initially get stronger as attached bacterial populations grow, but as the particle material becomes more refractory and the bacterial population declines the aggregate attachments might weaken.

The majority of the data presented were collected using tethered euphausiids. A stationary animal can create a more sustained, higher velocity flow field capable of drawing aggregates in from farther away (Emlet 1990). In this study, the effective radius of a tethered euphausiid, as defined by the average distance from which particles could be drawn in and fragmented, was 6.7 mm, almost twice as large as the 3.5-mm effective radius of free-swimming euphausiids determined by Dilling and Alldredge (2000) using bioluminescent dinoflagellates as a flow diagnostic (Rohr et al. 1997). However, the threshold shear stress for the dinoflagellate used was five times higher than that necessary to fragment many types of marine snow (Alldredge et al. 1990). With a critical stress of $\sim$0.15 dyn cm^{-2} (Alldredge et al. 1990), particle image velocimetry (PIV) data for free-swimming euphausiids indicated an effective radius of 3 cm for a 2-cm animal swimming at 10 cm s^{-1}. This value represents the maximum effective radius and compares favorably with data from tethered animals where the maximum distance at which particles fragmented was 3.7 cm.

Euphausiid effective radii likely depend on swimming mode. Three swimming modes have been described for *E. pacifica:* hovering at a fixed angle ($\sim$20°) and constant speed ($<$1 cm s^{-1}), hovering at variable angles ($\sim$30–50°) at alternating speeds (0–1 cm s^{-1}) while raising and lowering the head, and fast swimming ($>$1 cm s^{-1}) with great fluctuations in swimming angle (2 to $>$50°; Miyashita et al. 1996). The effective radius for a hovering animal is likely more similar to a tethered animal, whereas a rapidly swimming animal probably has a smaller effective radius similar to that predicted by the bioluminescence assay (Dilling and Alldredge 2000). The spatial region where most particles were fragmented, namely, near the pleopods, corresponds to the highest measured shear stress region for both free-swimming and tethered animals.

Larger animals will likely have a more dramatic effect on particle fragmentation due to their larger flow fields, faster swimming speeds, and greater extent of vertical migration. Euphausiids used in this experiment spanned the size range for adult *E. pacifica*. *E. pacifica* can form swarms with densities as high as 10,000 animals m^{-3} (Mackie and Mills 1983) and may school under certain circumstances such as daytime feeding during phytoplankton blooms (Komaki 1967; Hanamura et al. 1984). Schooling could enhance particle fragmentation, since proposed animal positioning in schools (Wiese and Ebina 1995) would result in daughter particles being passed down the fringes of the propulsion jet from one animal to the next. This process might be particularly dramatic for *Euphausia superba*, a much larger euphausiid, which is often found in schools in the Southern Ocean, where shelf regions are characterized by large diatom blooms. The nearest neighbor distance for schooling *E. superba* is $\sim$30 mm (Hamner and Hamner 2000), and these euphausiids likely have effective radii of at least 15 mm, since they are twofold to threefold larger than *E. pacifica.* Thus, any aggregate in the path of the large ($\sim$1500 m^3), quickly moving (20 cm s^{-1}) schools of *E. superba* would likely be fragmented. As shown in this study, euphausiids are also capable of fragmenting their own fecal pellets, although at lower rates than for marine snow aggregates. Fecal pellet fragmentation by swimming animals might be an important mechanism for fracturing the peritrophic membrane and releasing internal components. Fragmentation would also reduce sinking rates and might help to explain observations of sustained residence of fecal pellets in surface waters (Alldredge et al. 1987). Lampitt et al. (1990) also observed fecal pellet fragmentation through a different process called corprorhexy, whereby copepods removed and ingested only the peritrophic membrane of fecal pellets.

Since all euphausiids have a similar morphology, with five pairs of rapidly beating pleopods, all euphausiid species should be capable of fragmenting particles. Those euphausiids attaining large sizes and high abundances, such as *E. superba* in the Southern Ocean ($<$1–100,000 m^{-3}), *Meganyctiphanes norvegica* (0.1–1 m^{-3}) in the North Atlantic, *Nyctiphanes australis* ($<$1–5 m^{-3}) off Tasmania, *N. capensis* in the Benguela Current ($>$3–28 m^{-3}), and *Thysanoessa inermis* in the Barents Sea (0.1 to $>$1 m^{-3}; reviewed in Siegel 2000), might be particularly important in affecting particle flux. However, for this process to be significant, both euphausiids and marine snow need to be abundant. Euphausiids tend to be most abundant in upwelling, eutrophic regions (Siegel 2000), although they have global distribution. Those euphausiids inhabiting productive regions also tend to be larger in size. Marine snow is also most abundant in eutrophic regions, since phytoplankton and detrital material can form the bulk of large aggregates. It is in these productive regions where particle flux is high that fragmentation by swimming euphausiids would be most important. Using an average swimming speed of 1 cm s^{-1} (Torres and Childress 1983), an abundance range of 1–10 euphausiids m^{-3}, and the average effective radius determined in this study (6.7 mm), *E. pacifica* could interact with from $\sim$5% to 50% of the particles in the upper 100 m over an 8-h period. Euphausiids at densities $>$20 animals m^{-3} could interact with $>$100% of the particles. Similar impacts would be expected for the other euphausiids species listed above, which generally fall into the size range of *E. pacifica* tested in this study, except *E. superba,* which are much larger and, at similar densities, would affect a greater percentage of the water column.

There are likely many other macrozooplankton that are also capable of fragmenting aggregates. Pelagic shrimp and mysids have similar rapidly beating appendages. Organisms that move by jet propulsion such as medusae (Costello and Colin 1994) and salps (Bone and Trueman 1983) create high shear jets, which could fragment aggregates. Swimming

ctenophores have been noted to fragment larvacean houses in field observations (Steinberg et al. 1997). Also, copepods swimming at burst speeds can create shear stresses up to 45 dyn cm^{-2} (Morris et al. 1985; Latz et al. 1994), which are adequate to fragment marine snow (Alldredge et al. 1990).

This novel mechanism of fragmentation by swimming zooplankton is more apt to explain decreases in particle flux with depth than previous popular arguments of fragmentation by abiotic physical shear. Swimming of macrozooplankton provides a mechanism for fragmenting aggregates in the depth interval from 100 to 500 m, where the most dramatic losses of sinking particles occur. Many macrozooplankton are vertical migrators, rising from depths as great as 1000 m to the upper 100 m each night. With typical marine snow sinking rates of 20–200 m d^{-1} (Alldredge and Gotschalk 1988), migrators would have the opportunity to interact with a particle field over multiple nights in succession. Several studies of water column marine snow have shown a diel periodicity in aggregate abundance and total volume (Lampitt et al. 1993; Graham et al. 2000; Stemmann et al. 2000). Swimming of migrating macrozooplankton might help to explain these patterns. Fragmentation resulting from swimming behavior is a novel mechanism, since it maintains POC concentration while changing particle size structure. This alteration can have important consequences not only for flux but also for food size and availability to grazers in surface and deep waters. These impacts will be modeled in a subsequent paper.

References

ALLDREDGE, A. L. 1979. The chemical composition of macroscopic aggregates in two neretic seas. Limnol. Oceanogr. **24:** 855–866.

———. 1991. In situ collection and laboratory analysis of marine snow and large fecal pellets. Geophys. Monogr. **63:** 43–46.

———. 2000. Interstitial dissolved organic carbon (DOC) concentrations within sinking marine aggregates and their potential contribution to carbon flux. Limnol. Oceanogr. **45:** 1245–1253.

———, AND C. C. GOTSCHALK. 1988. In situ settling behavior of marine snow. Limnol. Oceanogr. **33:** 339–351.

———, T. C. GRANATA, C. C. GOTSCHALK, AND T. D. DICKEY. 1990. The physical strength of marine snow and its implications for particle disaggregation in the ocean. Limnol. Oceanogr. **35:** 1415–1428.

———, ———, AND S. MACINTYRE. 1987. Evidence for sustained residence of macrocrustacean fecal pellets in surface waters off Southern California. Deep-Sea Res. **34:** 1641–1652.

———, AND M. W. SILVER. 1988. Characteristics, dynamics and significance of marine snow. Prog. Oceanogr. **20:** 41–82.

ASPER, V. L. 1987. Measuring the flux and sinking speed of marine snow aggregates. Deep-Sea Res. **34:** 1–17.

BANSE, K. 1990. New views on the degradation and deposition of organic particles as collected by sediment traps in the open sea. Deep-Sea Res. **37:** 1177–1195.

BICKFORD, W. 1993. Mechanics of solids—concepts and applications. Irwin.

BONE, Q., AND E. R. TRUEMAN. 1983. Jet propulsion in salps. J. Zool. Lond. **201:** 481–506.

BRINTON, E. 1976. Population biology of *Euphausia pacifica* off Southern California. Fish. Bull. **74:** 733–762.

———, AND J. G. WYLLIE. 1976. Distributional atlas of euphausiid growth stages off southern California, 1953 through 1956. Calif. Coop. Ocean. Fish. Invest., Atlas **24:** 1–289.

BROOKS, E. R., AND M. M. MULLIN. 1983. Diel changes in the vertical distribution of biomass and species in the Southern California Bight. Calif. Coop. Ocean. Fish. Invest. Rep. **24:** 210–215.

BUCHANAN, G. 1988. Mechanics of materials. Holt, Rinehart, and Winston.

COSTELLO, J. H., AND S. P. COLIN. 1994. Morphology, fluid motion and predation by the schyphomedusa *Aurelia aurita.* Mar. Biol. **121:** 327–334.

DILLING, L., AND A. L. ALLDREDGE. 2000. Fragmentation of marine snow by swimming macrozooplankton: A new process impacting carbon cycling in the sea. Deep-Sea Res. I **47:** 1227–1245.

EMLET, R. B. 1990. Flow fields around ciliated larvae: Effects of natural and artificial tethers. Mar. Ecol. Prog. Ser. **63:** 221–225.

FOWLER, S. W., AND G. A. KNAUER. 1986. Role of large particles in the transport of elements and organic compounds through the oceanic water column. Prog. Oceanogr. **16:** 147–194.

GRAHAM, W. M., S. MACINTYRE, AND A. L. ALLDREDGE. 2000. Diel variations of marine snow concentration in surface waters and implications for particle flux in the sea. Deep-Sea Res. I **47:** 367–395.

HAMNER, W. M., AND P. P. HAMNER. 2000. Behavior of Antarctic krill (*Euphausia superba*): Schooling, foraging, and antipredatory behavior. Can. J. Fish. Aquat. Sci. **57:** 192–202.

HANAMURA, Y., Y. ENDO, AND A. TANIGUCHI. 1984. Underwater observations on the surface swarm of a euphausiid, *Euphausia pacifica* in Sendai Bay, Northeastern Japan. La Mer **22:** 63–69.

HILL, P. S. 1996. Sectional and discrete representations of floc breakage in agitated suspensions. Deep-Sea Res. I **43:** 679–702.

KARL, D. M., G. A. KNAUER, AND J. H. MARTIN. 1988. Downward flux of particulate organic matter in the ocean: A particle decomposition paradox. Nature **332:** 438–441.

KILPS, J. R., B. E. LOGAN, AND A. L. ALLDREDGE. 1994. Fractal dimensions of marine snow determined from image analysis of in situ photographs. Deep-Sea Res. I **41:** 1159–1169.

KIØRBOE, T. 2000. Colonization of marine snow aggregates by invertebrate zooplankton: Abundance, scaling, and possible role. Limnol. Oceanogr. **45:** 479–484.

KOMAKI, Y. 1967. On the surface swimming of euphausiid crustaceans. Pac. Sci. **21:** 433–448.

LAMPITT, R. S., W. R. HILLIER, AND P. G. CHALLENOR. 1993. Seasonal and diel variation in the open ocean concentration of marine snow aggregates. Nature **362:** 737–739.

———, T. NOJI, AND B. VON BODUNGEN. 1990. What happens to zooplankton fecal pellets? Implications for material flux. Mar. Biol. **104:** 15–23.

LASKER, R., AND G. H. THEILACKER. 1965. Maintenance of euphausiid shrimps in the laboratory. Limnol. Oceanogr. **9:** 287–288.

LATZ, M. I., J. F. CASE, AND R. C. GRAN. 1994. Excitation of bioluminescence by laminar fluid shear associated with simple Couette flow. Limnol. Oceanogr. **39:** 1424–1439.

LOGAN, B. E., AND D. B. WILKINSON. 1990. Fractal geometry of marine snow and other biological aggregates. Limnol. Oceanogr. **35:** 130–136.

MACKIE, G. O., AND C. E. MILLS. 1983. Use of the Pisces IV submersible for zooplankton studies in coastal waters of British Columbia. Can. J. Fish. Aquat. Sci. **40:** 763–775.

MARTIN, J. H., G. A. KNAUER, D. M. KARL, AND W. BROENKOW.

1987. VERTEX: Carbon cycling in the northeast Pacific. Deep-Sea Res. **34:** 267–285.

MAUCHLINE, J. 1980. The biology of euphausiids. Adv. Mar. Biol. **18:** 373–623.

MIYASHITA, K., I. AOKI, AND T. INAGAKI. 1996. Swimming behavior and target strength of isada krill (*Euphausia pacifica*). ICES J. Mar. Sci. **53:** 303–308.

MORRIS, M. J., G. GUST, AND J. J. TORRES. 1985. Propulsion efficiency and cost of transport for copepods: A hydromechanical model of crustacean swimming. Mar. Biol. **86:** 283–295.

PARKER, D. S., W. J. KAUFMAN, AND D. JENKINS. 1972. Floc break-up in turbulent flocculation processes. J. Sanit. Eng. Div. Am. Soc. Civ. Eng. **98:** 79–99.

PLOUG, H., AND H.-P. GROSSART. 1999. Bacterial production and respiration in suspended aggregates—a matter of the incubation method. Aquat. Microb. Ecol. **20:** 21–29.

———, AND ———. 2000. Bacterial growth and grazing on diatom aggregates: Respiratory carbon turnover as a function of aggregate size and sinking velocity. Limnol. Oceanogr. **45:** 1467–1475.

———, ———, F. AZAM, AND B. B. JORGENSEN. 1999. Photosynthesis, respiration, and carbon turnover in sinking marine snow from surface waters of Southern California Bight: Implications for the carbon cycle in the ocean. Mar. Ecol. Prog. Ser. **179:** 1–11.

RAFFEL, M., C. WILLERT, AND J. KOMPENHANS. 1998. Particle image velocimetry—a practical guide. Springer-Verlag.

ROHR, J., J. ALLEN, J. LOSEE, AND M. I. LATZ. 1997. The use of bioluminescence as a flow diagnostic. Phys. Lett. A **228:** 408–416.

RUIZ, J. 1997. What generates daily cycles of marine snow? Deep-Sea Res. I **44:** 1105–1126.

SCHLICHTING, H. 1979. Boundary-layer theory. McGraw-Hill.

SHANKS, A. L., AND E. W. EDMONDSON. 1989. Laboratory-made artificial marine snow: A biological model of the real thing. Mar. Biol. **101:** 463–470.

———, AND J. D. TRENT. 1979. Marine snow: Microscale nutrient patches. Limnol. Oceanogr. **24:** 850–854.

SHIGLEY, J., AND C. MISCHKE. 1989. Mechanical engineering design. McGraw Hill.

SIEGEL, V. 2000. Krill (Euphausiacea) demography and variability in abundance and distribution. Can. J. Aquat. Sci. **57:** 151–167.

STEINBERG, D. K., M. W. SILVER, AND C. H. PILSKALN. 1997. Role of mesopelagic zooplankton in the community metabolism of giant larvacean house detritus in Monterey Bay, California, USA. Mar. Ecol. Prog. Ser. **147:** 167–179.

STEMMANN, L., M. PICHERAL, AND G. GORSKY. 2000. Diel variation in the vertical distribution of particulate matter (>0.15 mm) in the NW Mediterranean Sea investigated with the Underwater Video Profiler. Deep-Sea Res. I **47:** 505–531.

STRICKLER, J. R. 1998. Observing free-swimming copepods mating. Philos. Trans. R. Soc. Lond. B **353:** 671–680.

TORRES, J. J., AND J. J. CHILDRESS. 1983. Relationship of oxygen consumption to swimming speed in *Euphausia pacifica.* I. Effects of temperature and pressure. Mar. Biol. **74:** 79–86.

TURNER, J. T. 2002. Zooplankton fecal pellets, marine snow and sinking phytoplankton blooms. Aquat. Microb. Ecol. **27:** 57–102.

VAN DUREN, L. A., E. J. STAMHUIS, AND J. J. VIDELER. 1998. Reading the copepod personal ads: Increasing encounter probability with hydromechanical signals. Philos. Trans. R. Soc. Lond. B **353:** 691–700.

———, ———, AND ———. 2003. Copepod feeding currents: Flow patterns, filtration rates and energetics. J. Exp. Biol. **206:** 255–267.

WESTERWEEL, J. 1997. Fundamentals of digital particle image velocimetry. Meas. Sci. Technol. **8:** 1379–1392.

WIESE, K., AND Y. EBINA. 1995. The propulsion jet of *Euphausia superba* (Antarctic krill) as a potential communication signal among conspecifics. J. Mar. Biol. Assoc. U.K. **75:** 43–54.

YEN, J., J. BROWN, AND D. R. WEBSTER. 2003. Analysis of the flow field of the krill, *Euphausia pacifica.* Mar. Freshw. Behav. Physiol. **36:** 307–319.

Received: 3 October 2003
Accepted: 11 February 2004
Amended: 5 March 2004